Journal of the American Heart Association

ORIGINAL RESEARCH

Impact of Right Ventricular-Pulmonary Circulation Coupling on Mortality in SARS-CoV-2 Infection

Francesca Bursi, MD, PhD, MSc; Gloria Santangelo, MD; Andrea Barbieri, MD; Anna Maria Vella, MD; Filippo Toriello, MD; Federica Valli, MD; Dario Sansalone, CCP; Stefano Carugo, MD; Marco Guazzi, MD, PhD

BACKGROUND: The COVID-19–related pulmonary effects may negatively impact pulmonary hemodynamics and right ventricular function. We examined the prognostic relevance of right ventricular function and right ventricular-to-pulmonary circulation coupling assessed by bedside echocardiography in patients hospitalized with COVID-19 pneumonia and a large spectrum of disease independently of indices of pneumonia severity and left ventricular function.

METHODS AND RESULTS: Consecutive COVID-19 subjects who underwent full cardiac echocardiographic evaluation along with gas analyses and computed tomography scans were included in the study. Measurements were performed offline, and quantitative analyses were obtained by an operator blinded to the clinical data. We analyzed 133 patients (mean age 69±12 years, 57% men). During a mean hospital stay of 26±16 days, 35 patients (26%) died. The mean tricuspid annular plane systolic excursion/pulmonary artery systolic pressure (TAPSE/PASP) ratio was 0.48±0.18 mm/Hg in nonsurvivors and 0.72±0.32 mm/Hg in survivors (P=0.002). For each 0.1 mm/mm Hg increase in TAPSE/PASP, there was a 27% lower risk of in-hospital death (hazard ratio [HR], 0.73 [95% CI, 0.59–0.89]; P=0.003). At multivariable analysis, TAPSE/PASP ratio remained a predictor of in-hospital death after adjustments for age, oxygen partial pressure at arterial gas analysis/fraction of inspired oxygen, left ventricular ejection fraction, and computed tomography lung score. Receiver operating characteristic analysis was used to identify the cutoff value of the TAPSE/PASP ratio, which best specified high-risk from lower-risk patients. The best cutoff for predicting in-hospital mortality was TAPSE/PASP <0.57 mm/mm Hg (75% sensitivity and 70% specificity) and was associated with a >4-fold increased risk of in-hospital death (HR, 4.8 [95% CI, 1.7–13.1]; P=0.007).

CONCLUSIONS: In patients hospitalized with COVID-19 pneumonia, the assessment of right ventricular to pulmonary circulation coupling appears central to disease evolution and prediction of events. TAPSE/PASP ratio plays a mainstay role as prognostic determinant beyond markers of lung injury.

Key Words: COVID-19 ■ echocardiography ■ right ventricular function ■ right ventricular-pulmonary circulation coupling ■ strain

SARS-CoV-2 is the primary determinant of the current pandemic of COVID-19 and has become a major public health concern. The disease exhibits a large variety of clinical severity ranging from asymptomatic infection to severe bilateral pneumonia with respiratory failure, eventually leading to death.[1]

SARS-CoV-2 may cause acute and chronic direct myocardial injury, or indirectly through cardiac stress because of hypoxemia, systemic inflammation, pulmonary parenchyma damage, or circulation involvement.[2] Understanding the pathophysiology of heart and lung interaction in this setting may be useful to clarify the

Correspondence to: Marco Guazzi, Division of Cardiology, Department of Health Sciences, San Paolo University Hospital, Azienda Socio Sanitaria Territoriale Santi Paolo e Carlo, University of Milan Medical School, Via Antonio di Rudinì 8, Milan, Italy. E-mail: marco.guazzi@unimi.it

Supplementary Material for this article is available at https://www.ahajournals.org/doi/suppl/10.1161/JAHA.121.023220.

For Sources of Funding and Disclosures, see page 11.

JAHA is available at: www.ahajournals.org/journal/jaha

CLINICAL PERSPECTIVE

What Is New?

- There is emerging evidence that COVID-19 may negatively impact pulmonary hemodynamics and right ventricular (RV) function.
- The relationship between tricuspid annular plane systolic excursion (longitudinal RV fiber shortening) and pulmonary artery systolic pressure (RV afterload) provides a noninvasive index of in vivo RV load adaptability that may unmask latent right heart disease in different clinical settings.
- In our cohort of hospitalized patients with COVID-19 pneumonia, we assessed the independent prognostic relevance of RV to pulmonary circulation coupling performed by bedside echocardiography assessed along with markers of lung injury and left ventricular function; tricuspid annular plane systolic excursion/pulmonary artery systolic pressure ratio appears as an independent marker of disease evolution and prediction of in-hospital death.

What Are the Clinical Implications?

- Although underlying mechanisms for these associations are not fully understood, tricuspid annular plane systolic excursion/pulmonary artery systolic pressure ratio might be part of a multiparametric clinical evaluation to identify high-risk patients and optimize management of patients with COVID-19.
- Prespecified studies would be of interest for understanding how much these echocardiographic results can impact on patient management and clinical decision making.

Nonstandard Abbreviations and Acronyms

GLS	global longitudinal strain
LS	longitudinal strain
PASP	pulmonary artery systolic pressure
Pc	pulmonary circulation
TAPSE	tricuspid annular plane systolic excursion

hemodynamic consequences of pneumonia and help to tailor adequate therapy for multifold targets.

Acute right heart failure is a known complication of acute respiratory distress syndrome (ARDS) attributable to other diseases, and there is emerging evidence of right ventricular (RV) dysfunction in patients with COVID-19.[3,4] However, results are controversial, and studies have been chiefly limited to patients with the most severe disease presentation.[5,6] Our group and others observed that RV strain was frequently abnormal and provided independent prognostic value over markers of lung disease.[7,8] Further exploration of RV function by addressing its coupling with pulmonary circulation (Pc) appears quite attractive and may reveal latent right heart disease with more solid perspectives on prognosis and clinical evolution.

Accordingly, our primary aim was to systematically assess the value of RV-to-Pc coupling and right heart failure by bedside echocardiography in predicting all-cause death among hospitalized patients with COVID-19 pneumonia presenting with a wide variety of disease severity.

METHODS

We analyzed all patients diagnosed with COVID-19 who underwent a clinically indicated echocardiogram in 2020 and were admitted to regular or subintensive or intensive care wards at the San Paolo University Hospital of Milan, Lombardy region, the area most affected by the pandemic in Italy at the time the study was conducted.

Study methods have been outlined before.[7] Briefly, according to the World Health Organization guidance, the diagnosis of SARS-CoV-2 infection was confirmed as a positive result of real-time reverse transcriptase–polymerase chain reaction assay of nasal and pharyngeal swabs. The institutional ethics board of Azienda Socio Sanitaria Territoriale Santi Paolo e Carlo Santi Paolo and Carlo, Milan, approved this study (protocol number 2020/ST/099). Patients provided informed consent for data use.

At the time of data collection, no vaccine was available.

Baseline clinical characteristics, laboratory, radiological, and instrumental data as well as therapy were obtained by review of electronic medical records. We collected arterial blood gases analysis, type of ventilator support, and vital parameters at the time of the echocardiographic exam. Data were used to calculate the Sequential Organ Failure Assessment score.[9] ARDS was defined by applying the Berlin criteria.[10] The time to echocardiogram was the time lag from hospital admission to the day of the echocardiogram.

All laboratory exams were collected at the time of the echocardiogram. C-reactive protein (CRP), high-sensitivity troponin I, and N-terminal pro-B-type natriuretic peptide (NT-proBNP) were collected also at the peak level. The Chronic Kidney Disease Epidemiology Collaboration equation was used to determine the estimated glomerular filtration rate.[11]

Computed tomography (CT) reports and images were reviewed in parallel to evaluate and confirm the typical COVID-19 features. A semiquantitative lung total severity score was calculated according to Chung

et al. Each of the 5 lung lobes was assessed for degree of involvement and classified as none (0%), minimal (1%–25%), mild (26%–50%), moderate (51%–75%), or severe (76%–100%), with a score of 0 to 4 for each segment. The overall lung total severity score was reached by summing the 5 lobe scores (range, 0–20) with higher values indicating a more significant alteration of lung parenchyma.[12]

In-hospital death was the outcome. Patients were followed-up from presentation to death or hospital discharge. The final enrollment date was December 15, 2020, the final follow-up date was January 13, 2021. The secondary end point was in-hospital death following the echocardiogram, and patients were followed to death or discharge.

Echocardiographic Exam

The echocardiograms were performed at the bedside, with patients in the left lateral decubitus position when possible, but mostly in a supine or sitting position with a machine dedicated to patients with COVID-19 (Vivid S6 echocardiograph; General Electric Medical System, Milwaukee WI). Personnel were provided with adequate personal protective equipment. To reduce the scan time, the exam was focused on answering the clinical problem according to international societies' recommendations.[13,14] The operator was required to store basic views, color Doppler imaging of the valves, and spectral continuous wave Doppler of the tricuspid regurgitant jet. Images were stored in a cine loop on the institutional server, and all measurements were performed off-line (EchoPAC version 203; General Electric Vingmed Ultrasound AS) according to current guidelines[15] by an expert operator blinded to the clinical data. Conventional parameters included RV fractional area change, tricuspid annular plane systolic excursion (TAPSE), maximum right atrio-ventricular trans-tricuspid gradient 4*(tricuspid regurgitation velocity).[2] We used inferior vena cava size changes to estimate right atrial pressure in patients not on positive expiratory pressure; this was added to the former to derive the pulmonary artery systolic pressure (PASP). In patients in whom inferior vena cava could not be used (positive airway pressure, insufficient quality of subcostal images) or in case of uncertainties, right atrial pressure was assumed to be 8 mm Hg according to guidelines.[16] TAPSE/PASP ratio was calculated as a surrogate of right ventriculoarterial coupling.[17] Left ventricular end-systolic volume and left ventricular ejection fraction (LVEF) were assessed using the Simpson biplane method. When volumes were not measurable, LVEF was visually estimated. Left atrial volume was measured with the biplane Simpson method and indexed to body surface area.[18] When the image quality allowed, longitudinal strain (LS) measurements were obtained by a single examiner according to the international society recommendations.[19] RV global longitudinal strain (RV-GLS) and longitudinal strain of the RV free-wall LS were measured from the apical 4-chamber view, and an endocardial border was traced delineating a region of interest. The software generated LS curves for each segment, and peak strain was calculated by averaging the values of each segment. To calculate the left ventricular (LV) LS, the endocardial border was manually traced in apical 4-, 2-, and 3-chamber views. After generating longitudinal curves by the software, the peak negative value was obtained by averaging the LV LS across all 17 segments. Similarly, left atrial peak LS was measured at the end of the reservoir phase by averaging the curves obtained from each segment from 4- and 2-chamber views. Segments in which adequate tracking quality was impossible despite manual adjustments were excluded from the analysis, and the strain parameters were obtained by averaging the remaining segments. To further explore the role of RV-to-Pc in this population, we calculated the RV free-wall LS and RV-GLS to PASP ratios.

Statistical Analysis

Values are expressed as mean±SD, as median and first and third quartile (Q1–Q3) in cases of highly skewed variables, or as percentages for categorical variables. Differences between groups were analyzed using an independent-sample t test, paired t test, Mann-Whitney test, χ^2, or Fisher exact test as appropriate. Correlations between variables were evaluated with Pearson coefficients, and highly skewed variables were log transformed.

Cox proportional hazards model analysis was used to calculate the risk of death; data are presented as hazard ratios (HRs) and 95% CIs. Multiple Cox proportional hazards models of multivariable adjustments were performed to examine the prognostic role of RV coupling by adjusting for relevant markers of prognosis and lung involvement. Model 1 adjusted for age and oxygen partial pressure at arterial gas analysis/fraction of inspired oxygen (PaO_2/FiO_2). Model 2 adjusted for age, PaO_2/FiO_2, and ejection fraction. Model 3 adjusted for age, PaO_2/FiO_2, and CT lung score. PaO_2/FiO_2 was considered as a marker of abnormal function of the lung, CT lung score as a marker of extension of anatomical involvement of the lung, and ejection fraction as a marker of LV dysfunction.

The variables were chosen by the investigator based on clinical relevance and significance at univariate analyses and entered in the Cox model. The model was kept as parsimonious as possible to avoid overfitting of the model. Bootstrap validation was performed across 1000 bootstrapped replicates to evaluate the stability of the prediction model. A stepwise backward

regression model was set up from all parameters that were predictive at univariable analysis to identify the optimal combination of predictive variables (age, previous cardiac disease, CT lung severity score, PaO_2/FiO_2, LVEF, and TAPSE/PASP ratio). A χ^2 test comparing the log likelihood ratios of nested models was obtained to evaluate the model predictive performance of TAPSE and PASP alone or as a ratio.

To evaluate the prognostic accuracy of RV-to-Pc coupling in predicting in-hospital death, receiver operating characteristic (ROC) curves were constructed, the area under the curve (AUC) was calculated, and sensitivity and specificity were calculated using standard definitions. ROC analysis was used to identify the cutoff value of the TAPSE/PASP ratio that best identified higher- and lower-risk patients. The cutoff was the value corresponding to the greatest combination of sensitivity and specificity.

Kaplan-Meier analysis was used to depict survival stratified by TAPSE/PASP best cutoff, and the 2 groups were compared using the log-rank test. Absolute values of LV LS, RV-GLS, and free-wall LS were used in the analyses for simpler interpretation. Analyses were performed using the Statistical Package for the Social Sciences version 23 (IBM, Armonk, NY), and a 2-sided value of $P<0.05$ was considered statistically significant.

The data that support the findings of this study are available from the corresponding author upon reasonable request.

RESULTS

Population Characteristics

The study population consisted of 133 patients; the mean age was 69±12 years, 57% were men, and 83% were White. The indications for the exam were suspected right heart dysfunction in 20%, left heart or valve dysfunction in 31%, monitor of known cardiac disease in 17%, suspected endocarditis in 13%, pericardial effusion in 5%, stroke in 1%, and other reasons in 14%. At the time of the echocardiographic exam, 12 (9%) patients were intubated, 4 (3%) were in bilevel positive airway pressure, 44 (33%) in continuous positive airway pressure, 34 (26%) in face mask with high oxygen flow, 20 (15%) in nasal cannula, and 11 (14%) in room air. The mean sequential organ failure assessment was 2.3±1.9; 48% of patients met the Berlin criteria for ARDS, and mean PaO_2/FiO_2 was 249±134 mm Hg. Pulmonary involvement by CT showed a total severity lung score of 9±6; in 8 patients a concomitant segmental pulmonary embolism diagnosis was made. Contrast-enhanced CT for pulmonary embolism diagnosis was performed in a similar proportion in survivors (30%) and nonsurvivors (27%) ($P=0.759$). Median (Q1–Q3) CRP was 102 mg/L (56–126 mg/L), procalcitonin was 0.34 ng/mL (0.10–1.342 ng/mL), lymphocytes 9% per µL (5%–16% per µL), neutrophils 84% per µL (73%–90% per µL), and D-dimer 1119 ng/mL (462–2975 ng/mL). Mean estimated glomerular filtration rate was 71±32 mL/min per 1.73 m^2. Troponin I was measured in 53% and was only mildly elevated, and the median (Q1–Q3) was 0.08 ng/dL (0.01–0.21 ng/dL). NT-proBNP was available in 58 patients, and the median (Q1–Q3) value was 2925 pg/mL (586–8857 pg/mL) (Table 1).

Clinical and Echocardiographic Characteristics of Survivors and Nonsurvivors

During a mean hospital stay of 26±16 days, 35 (26%) patients died. Table 1 shows the characteristics of the entire population and of survivors versus nonsurvivors. Nonsurvivors were older, had a higher prevalence of cardiac diseases, showed worse respiratory parameters, and had a worse index of multiorgan failure. At the CT they presented a worse calculated lung severity score and higher CRP levels, whereas they were similar for other laboratory parameters, cardiovascular risk factors distribution, and primary COVID-19 therapies (Table 1). Echocardiography was performed at a median (Q1–Q3) of 8 (3–14) days from the diagnosis, 9 (5–17) days in survivors versus 5 (3–11) days in nonsurvivors ($P=0.006$).

Despite having similar indexed LV volumes and RV size, nonsurvivors showed significantly worse echocardiographic paraments of LV and RV systolic function than survivors. Notably, they presented worse indices of LV systolic dysfunction, including lower LVEF, higher wall motion score index, and worse LV-GLS, as well as lower peak left atrial longitudinal strain. Remarkably, nonsurvivors had significantly worse RV parameters, higher PASP, worse RV indices of longitudinal function including decreased TAPSE, and when it was measurable, a worse RV-GLS and free-wall LS. Consequently, they showed worse indices of RV-to-Pc coupling. The mean TAPSE/PASP ratio was 0.48±0.18 in nonsurvivors and 0.72±0.32 mm/Hg in survivors ($P<0.002$) (Table 2).

RV-to-Pc coupling was associated with in-hospital death. For each 0.1 mm/mm Hg increase in TAPSE/PASP, there was a 27% lower risk of in-hospital death (HR, 0.73 [95% CI, 0.59–0.89]; $P=0.003$). In a series of multivariable models, the association of TAPSE/PASP ratio and in-hospital death remained after adjustments for age, PaO_2/FiO_2, LVEF, and CT lung score. (Table 3) The internal validity of these models was confirmed by bootstrapping (all $P<0.004$). To confirm the robustness of our results we examined the incremental value of TAPSE/PASP ratio. The likelihood ratio tests between nested models showed that adding TAPSE/PASP to the models including age, PaO_2/FiO_2, and TAPSE and age, PaO_2/FiO_2, and PASP improved the models significantly (both $P<0.05$).

Table 1. Characteristics of Study Patients by In-Hospital Mortality

Variable	Feasibility, %	Total, 133	Survivors, 98	Nonsurvivors, 35	*P* value
Age, y	100	69±12	67±13	76±11	<0.001
Male sex, n (%)	100	76 (57)	58 (59)	18 (51)	0.426
Weight, kg	95	75±16	76±17	73±15	0.336
BSA, m^2	95	1.8±0.2	1.9±0.2	1.8±0.2	0.303
White race, n (%)	100	112 (83)	80 (82)	32 (94)	0.172
Risk factors and history					
Smoking, n (%)	100	35 (26)	23 (23)	12 (34)	0.475
Hypertension, n (%)	100	77 (58)	54 (55)	23 (65)	0.275
Diabetes, n (%)	100	32 (24)	22 (22)	10 (29)	0.467
Previous cardiac disease, n (%)	100	50 (38)	30 (31)	20 (57)	0.005*
History of coronary disease, n (%)	100	29 (22)	16 (16)	13 (37)	0.010*
History of heart failure, n (%)	100	12 (9)	5 (5)	7 (20)	0.008*
Previous valve disease, n (%)	100	15 (11)	6 (6)	9 (26)	0.004*
Atrial fibrillation, n (%)	100	21 (16)	13 (13)	8 (22)	0.182
ACE inhibitors or ARB before admission, n (%)	99	55 (42)	36 (37)	19 (54)	0.078
History of cancer, n (%)	100	18 (13)	12 (12)	6 (17)	0.565
Chronic obstructive pulmonary disease, n (%)	100	20 (15)	12 (12)	8 (23)	0.132
Previous stroke, n (%)	100	10 (8)	4 (4)	6 (17)	0.021*
In-hospital therapy					
Corticosteroids, n (%)	100	85 (64)	63 (65)	22 (67)	0.858
Prophylactic anticoagulants, n (%)	100	61 (46)	49 (50)	12 (34)	0.274
Therapeutic anticoagulants, n (%)		62 (47)	42 (43)	20 (57)	
Hydroxychloroquine, n (%)	100	37 (28)	29 (30)	8 (23)	0.445
Monoclonal antibodies, n (%)	100	4 (3)	3 (3)	1 (3)	0.952
Antivirals, n (%)	100	24 (18)	19 (19)	5 (14)	0.500
Immunosuppressants, n (%)	100	4 (3)	4 (4)	0	0.225
Antibiotics, n (%)	100	93 (70)	67 (68)	26 (74)	0.512
Presentation					
ARDS by Berlin criteria, n (%)	100	53 (48)	34 (35)	19 (54)	0.047*
Type of ventilation, n (%)	100				0.381
None		19 (14)	16 (16)	3 (9)	
Nasal cannula		20 (15)	14 (14)	6 (17)	
Face mask		34 (26)	27 (27)	7 (20)	
CPAP		44 (33)	32 (33)	12 (34)	
Bilevel		4 (3)	3 (3)	1 (3)	
Intubated		12 (9)	6 (6)	6 (17)	
CT total lung severity score	85	9±6	8±6	11±6	0.007*
SOFA score	86	2.3±1.9	2.1±1.9	2.9±1.7	0.062
Heart rate, bpm	100	83±15	82±15	88±14	0.028*
Respiratory rate, breaths per min	92	21±6	20±5	23±7	0.003*
Systolic blood pressure, mm Hg	100	129±24	129±21	126±27	0.420
Diastolic blood pressure, mm Hg	100	74±13	75±14	70±11	0.035*
Pulmonary embolism, n (%)	99	8 (6)	8 (8)	0	0.109

(*Continued*)

Table 1. (Continued)

Variable	Feasibility, %	Total, 133	Survivors, 98	Nonsurvivors, 35	*P* value
Laboratory data					
Oxygen saturation, %	100	96±3	97±3	94±4	0.001*
PaO_2/FiO_2, mm Hg	92	249±134	266±137	205±116	0.015*
PaO_2, mm Hg	91	112±55	121±59	87±32	<0.001*
FiO_2, %	96	50±22	49±22	53±24	0.378
pCO_2, mm Hg	90	39±8	39±7	39±11	0.9
pH	90	7.4±0.1	7.4±0.1	7.4±0.1	0.325
Creatinine, mg/dL, reference range 0.52–1.04	100	0.7 (0.6–1.1)	0.7 (0.6–0.9)	0.9 (0.7–1.7)	0.006*
eGFR, mL/min	100	71±32	87±32	65±31	0.001*
Lymphocytes, $\times 10^3/\mu L$, reference 1-3.4 $\times 10^3/\mu L$	100	1.4 (0.8–1.5)	1.2 (0.8–1.5)	1.0 (0.5–1.3)	0.035*
Lymphocytes, %, reference range 27–37	100	13 (9–23)	16 (11–26)	9 (5–14)	<0.001*
Neutrophils, $\times 10^3/\mu L$, reference range 1.5–7.5	100	5.9 (4.0–8.9)	4.9 (3.4–7.4)	8.0 (5.2–11.4)	<0.001*
Neutrophils, %, reference range 44–74	100	76 (64–84)	72 (62–83)	83 (75–90)	0.004*
AST, U/L, reference range 17–50	100	32 (25–49)	31 (24–45)	34 (26–54)	0.218
ALT, U/L, reference <50	100	28 (18–48)	29 (18–55)	24 (17–36)	0.208
Ferritin, ng/mL	75	484 (185–922)	447 (177–922)	666 (267–960)	0.249
D-dimer, ng/mL, reference <270	78	624 (326–1412)	586 (305–1155)	894 (527–2121)	0.099
Peak D-dimer, ng/mL	95	1119 (462–2975)	849 (398–2663)	1620 (1031–2980)	0.043*
Troponin I, ng/dL, reference <0.034	53	0.02 (0.01–0.13)	0.01 (0.01–0.08)	0.12 (0.01–0.41)	0.039*
Peak troponin I, ng/dL	53	0.08 (0.01–0.21)	0.04 (0.01–0.16)	0.18 (0.08–0.67)	0.014*
NT-proBNP, pg/mL, reference range 0–296	40	1560 (621–9127)	1106 (442–7745)	5800 (2585–13 825)	0.012*
Peak NT-proBNP, pg/mL	48	2925 (586–8857)	1550 (326–7850)	6520 (3130–14 250)	0.006*
CRP, mg/L, reference <10	100	40 (20–82)	34 (17–69)	79 (47–120)	<0.001*
Peak CRP, mg/L	100	102 (56–126)	91 (48–124)	123 (97–132)	0.002*
Duration of hospitalization, days	100	27±16	29±16	19±11	<0.001*

Data are presented as mean±SD, median (Q1–Q3), or number (percentage). Laboratory exams were collected at the time of the echocardiogram unless otherwise specified. ACE indicates angiotensin-converting enzyme; ALT, alanine aminotransferase; ARB, angiotensin receptor blocker; AST, aspartate aminotransferase; BSA, body surface area; CPAP, continuous positive airway pressure; CRP, C-reactive protein; CT, computed tomography; eGFR, estimated glomerular filtration rate; FiO_2, fraction of inspired oxygen; LVEF, left ventricular ejection fraction; NT-proBNP, N-terminal pro-B-type natriuretic peptide; PaO_2, oxygen partial pressure at arterial gas analysis; pCO2, partial pressure of carbon dioxide; Q1, first quartile; Q3, third quartile; and SOFA, sequential organ failure assessment.

*Indicates statistical significance.

In a stepwise backward multivariable regression analysis considering age, previous cardiac disease, CT lung severity score, PaO_2/FiO_2, and LVEF, the TAPSE/PASP ratio was retained in the model and was significantly associated with in-hospital death (adjusted HR for each 0.1 increase, 0.66 [95% CI, 0.51–0.84]; *P*=0.001). In a separate multivariable model after adjusting for D-dimer levels, TAPSE/PASP ratio remained associated with increased risk of death (for each 0.1 unit increase adjusted HR, 0.72 [95% CI, 0.56–0.93]; *P*=0.012).

An ROC analysis the AUC for in-hospital death for TAPSE was 0.68 (95% CI, 0.55–0.81; *P*=0.017), for PASP was 0.71 (95% CI, 0.59–0.83; *P*=0.005), and for the TAPSE/PASP ratio was 0.75 (95% CI, 0.64–0.86; *P*=0.001). The best cutoff for predicting in-hospital mortality was a TAPSE/PASP ratio <0.57 mm/mm Hg (75% sensitivity and 70% specificity) (Figure S1). The Figure shows the in-hospital survival curves by TAPSE/PASP best cutoff. Patients with TAPSE/PASP ratio <0.57 had a >4-fold increased risk of in-hospital death (HR, 4.8 [95% CI, 1.7–13.1]; *P*=0.003). Multivariable analyses showed the strength and significance of this association remained unaltered (Table 3). Baseline characteristics by the TAPSE/PASP best cutoff are shown in Table S1.

Table 2. Echocardiographic Characteristics in Survivors and Nonsurvivors

Echocardiographic data	Feasibility, %	Total, 133	Survivors, 98	Nonsurvivors, 35	*P* value
LVEDV index to BSA, mL/m^2	89	50±19	49±19	55±21	0.156
LVESV index to BSA, mL/m^2	85	25±16	24±16	28±18	0.168
LVEF, %	100	55±11	56±11	50±13	0.003*
WMSI	100	1.1±0.4	1.1±0.3	1.4±0.5	0.004*
LV GLS, %	53	16±4	16±4	12±5	0.002*
LAVi, mL/m^2	92	36±20	34±22	43±17	0.050
Left atrial peak longitudinal strain, %	66	19±9	20±9	15±9	0.039*
RV diameter, mm	83	35±6	35±5	36±7	0.188
FAC, %	79	41±7	41±6	38±8	0.110
Right atrial-ventricular gradient, mm Hg	68	28±11	26±10	34±11	0.003*
PASP, mm Hg	68	36±12	34±12	42±12	0.004*
Pulmonary valve acceleration time, ms	32	87±26	88±27	84±22	0.657
S′ tricuspid lateral annulus, ms	40	11±3	12±3	11±3	0.278
TAPSE, mm	89	21±5	22±4	19±4	0.001*
TAPSE/PASP, mm/mm Hg	65	0.66±0.31	0.72±0.32	0.48±0.18	0.002*
TAPSE/right atrial-ventricular gradient, mm/mm Hg	65	0.87±0.48	0.96±0.50	0.59±0.31	0.003*
RV GLS, %	57	15±4	16±4	12±4	<0.001*
RV free-wall strain, %	57	18±5	19±5	14±5	<0.001*
RV GLS/PASP, %/mm Hg	44	0.50±0.25	0.56±0.25	0.33±0.25	<0.001*
RV free wall strain/PASP, %/mm Hg	45	0.59±0.31	0.66±0.31	0.40±0.19	<0.001*
RAVi, mL/m^2	89	35±21	35±19	36±28	0.940

Strain parameters are presented as absolute values. BSA indicates body surface area; FAC, fractional area change; GLS, global longitudinal strain; LAVi, left atrial volume indexed; LV, left ventricular; LVEDV, left ventricular end diastolic volume; LVEF, left ventricular ejection fraction; LVESV, left ventricular end-systolic volume; PASP, pulmonary arterial systolic pressure; RAVi, right atrial volume indexed; RV, right ventricular; TAPSE, tricuspid annular plane systolic excursion; and WMSI, wall motion score index.

*Indicates statistical significance.

RV-to-Pc Coupling Correlates With Heart and Lung Parameters

The TAPSE/PASP ratio was significantly correlated with CT total lung severity score (r=−0.25, P=0.033) and with respiratory rate (r=−0.25, P=0.031), but was not related to PaO_2/FiO_2, sequential organ failure assessment, estimated glomerular filtration rate, D-dimer, and CRP. We observed a correlation with indices of myocardial injury in the 48 patients for whom high-sensitivity troponin I was available. After natural logarithmic (ln) transformation, the correlation with troponin showed r=−0.394, P=0.006. In the 38 patients in whom it was measured, lnNT-proBNP showed a good correlation with TAPSE/PASP ratio (r=−0.60, P<0.001).

As expected, there was a significant correlation between TAPSE/PASP ratio and LVEF (r=0.45, P<0.001), wall motion score index (r=−0.44, P<0.001), LV GLS (r=0.34, P<0.001), peak left atrial LS (r=0.51, P<0.001), and left atrial volume indexed (r=−0.26, P=0.017). In

Table 3. Univariate and Multivariable Cox Proportional Hazard Models for TAPSE/PASP and Risk of In-Hospital Mortality

	HR for 0.1 mm/mm Hg TAPSE/PASP increase (95% CI)	*P* value	HR for TAPSE/PASP <0.57 (95% CI)	*P* value
Unadjusted model, N=86	0.73 (0.59–0.89)	0.003	4.7 (1.7–13.1)	0.007
Model 1: adjusted for age and PaO_2/FiO_2, N=81	0.66 (0.52–0.84)	0.001	6.3 (2.0–19.0)	0.001
Model 2: adjusted for age, PaO_2/FiO_2, and LVEF, N=81	0.71 (0.55–0.93)	0.012	4.6 (1.3–16.8)	0.016
Model 3: adjusted for age, PaO_2/FiO_2, and CT lung score, N=69	0.72 (0.54–0.94)	0.017	4.8 (1.5–15.8)	0.009

CT indicates computed tomography; FiO_2, fraction of inspired oxygen; HR, hazard ratio; LVEF, left ventricular ejection fraction; PaO_2, oxygen partial pressure at arterial gas analysis; PASP, pulmonary arterial systolic pressure; and TAPSE, tricuspid annular plane systolic excursion.

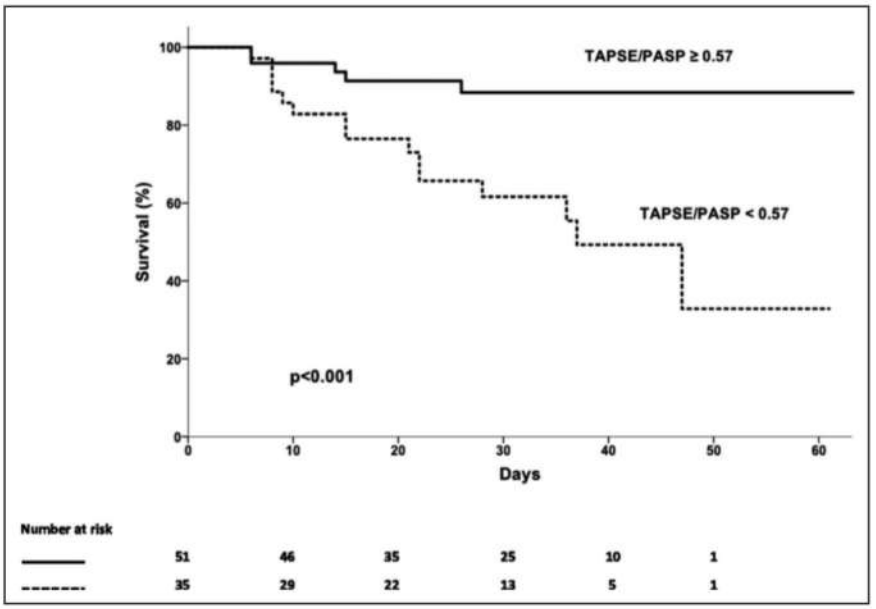

Figure. Kaplan Meier curve of percent of in-hospital survival stratified by TAPSE/PASP <0.57 mm/mm Hg or ≥0.57 mm/mm Hg.
PASP indicates pulmonary arterial systolic pressure; and TAPSE, tricuspid annular plane systolic excursion.

addition, TAPSE/PASP ratio was also correlated with RV echocardiographic variables such as fractional area change (r=0.40, P<0.001), RV-GLS (r=0.41, P=0.001), and RV free-wall LS (r=0.46, P<0.001). There was no correlation between time of echocardiogram and either TAPSE/PASP ratio or TAPSE and PASP alone (P>0.05).

Subgroup With a Pre–COVID-19 Echocardiogram

Thirty-four patients had an echocardiogram performed before COVID-19 infection. A significant correlation between the LVEF measured before and during COVID-19 pneumonia (r=0.73, P<0.001) was found. The mean LVEF before COVID was similar to that measured during COVID-19 pneumonia (54%±12% versus 55%±10%, P=not significant). Interestingly, this was not the case for the TAPSE/PASP ratio in the 15 patients with a pre–COVID-19 measurable TAPSE/PASP (r=0.23, P=0.44). The average TAPSE/PASP ratio was significantly higher before COVID (0.66±0.2 mm/mm Hg) compared with that measured during COVID-19 infection (0.47±0.2 mm/mm Hg) (P=0.013).

Sensitivity Analyses

There was a strong linear positive correlation between TAPSE/PASP and TAPSE/right atrio-ventricular gradient (r=0.974, P<0.0001). Interestingly, both variables provided similar results as reported in Table S2. At ROC analysis, the AUC for in-hospital death for TAPSE/right atrio-ventricular gradient was almost identical to that TAPSE/PASP ratio (0.75 [95% CI, 0.64–0.87]; P=0.001).

In the subgroup of patients for whom the quality of images was sufficient for RV speckle tracking analysis, RV-to-Pc was examined also as RV GLS/PASP and RV free-wall LS/PASP ratios. These were found to be significantly lower in nonsurvivors compared with patients discharged alive. (Table 2).

A good correlation has been observed between TAPSE/PASP and both RV-GLS/PASP and RV free-wall LS/PASP ratios (r=0.80, P<0.001 and r=0.81, P<0.001, respectively).

For each increase in 0.1 units of RV-GLS/PASP, there was a 35% reduced risk of in-hospital death (HR, 0.65 [95% CI, 0.50–0.85]; P=0.002; AUC, 0.77 [95% CI, 0.64–0.89]; P=0.002) and for each 0.1 unit increase in RV-free wall LS/PASP there was a 34% reduced risk of death (HR, 0.66 [95% CI, 0.51–0.86]; P=0.002; AUC, 0.78 [95% CI, 0.65–0.91]; P=0.001) (Figures S2 and S3). The best cutoff for predicting in-hospital mortality was a value of <0.51 for RV-GLS/PASP (94% sensitivity and 59% specificity) and of <0.49 for RV-free wall LS (87% sensitivity and 70% specificity). In the multivariable analysis after adjustments for age, previous cardiac disease, and CT lung severity score, PaO_2/FiO_2, LVEF, the RV GLS/PASP and the free-wall LS/PASP remained associated with in-hospital death (adjusted HR, 0.63 [95% CI, 0.45–0.87]; P=0.006 and adjusted HR, 0.67 [95% CI, 0.50–0.90]; P=0.008, respectively).

After excluding the 8 patients diagnosed with pulmonary embolism, the results were similar (data not shown).

DISCUSSION

The main findings of the present investigation were: (1) A latent RV-to-Pc uncoupling, estimated by TAPSE/PASP ratio, is common in hospitalized patients with COVID-19 pneumonia presenting with a wide variety of disease severity. (2) The TAPSE/PASP ratio is independently associated with an increased risk of in-hospital mortality, a finding that expands further the remarkable usefulness of this variable in daily clinical practice.

Insights on RV-to-Pc Coupling by TAPSE/PASP Ratio

The concept of ventriculo-arterial coupling refers to the relationship between ventricular contractility and afterload. The adequacy of RV contractility adaptation to afterload or coupling between the RV and the Pc occurs when there is a maximum transfer of potential energy from one elastic chamber (the ventricle) to another (the arterial system) at a minimal energy cost.[20] When contractility can no longer match afterload, a maladaptive remodeling with progressive RV dilation is required to ensure stroke volume through Frank-Starling mechanisms. This occurs at the expenses of increased filling pressures and, ultimately, clinical decompensation.[21] To detect these changes, we used a bedside transthoracic echocardiography surrogate of RV-to-Pc coupling, the TAPSE/PASP ratio, previously shown to be a valid correlate of invasively measured end-systolic to arterial elastance,[17,22] with TAPSE considered as a load-dependent surrogate of end-systolic elastance and PASP as an indirect estimate of arterial elastance. Remarkably, the TAPSE/PASP ratio has been proven to implement the prognostic accuracy in many clinical settings, such as chronic heart failure, with either reduced or preserved ejection fraction,[23–25] pulmonary arterial hypertension,[26] and pulmonary embolism.[27]

TAPSE/PASP provided superior prognostic importance than right ventricular function (TAPSE) alone or PASP alone, suggesting, in agreement with previous reports,[6] that it is not a mere ratio of 2 main effects that could be modeled independently, but rather, it is a useful independent measurement that provides greater prognostic information.

Clinical Implications of RV-to-Pc Uncoupling in COVID-19

There is a solid background for considering COVID-19 pneumonia a trigger of RV-to-Pc uncoupling. Uncoupling occurs in severe or rapidly evolving pulmonary vascular disease,[28] in severe inflammatory conditions such as sepsis,[29] or in left heart failure, a condition in which early RV-to-Pc uncoupling can be observed because of negative ventricular interactions.[30] In patients with COVID-19, similar substrates may be at work and contribute to a worse prognosis. We found that, despite a preserved RV size and function measured as fractional area change, some degree of RV-to-Pc uncoupling occurs and signals an increased risk of in-hospital death independently of age, PaO_2/FiO_2 ratio, and CT lung score.

There are several mechanisms through which the SARS-CoV-2 infection may impair the TAPSE/PASP ratio,[31] that is, a direct alveolar–capillary damage and consequent fibrosis promoting an inflammatory-driven microvessel disease,[32] which yields to an increased pulmonary vascular resistance, pulmonary vascular thrombosis, and embolism,[33] a negative inotropic effect mediated by the cytokine cascade and a direct myocardial injury.[34]

In the lung, the angiotensin-converting ezyme 2 vehicles SARS-CoV-2 favoring injury[35] and vasoconstriction, edema, and disrupted microvascular lung wall properties.[20] The sudden increase in RV afterload with the development of severe ARDS/hypoxemia and/or a poor RV function adaptation by direct myocardial injury/infarction[36] may contribute to a poor outcome. Although the role of one mechanism versus the other cannot be definitively dissected, some considerations are in order. The TAPSE/PASP ratio was significantly but weakly correlated with the severity of lung involvement by CT, and no association was found with markers of illness severity, including PaO_2/FiO_2, sequential organ failure assessment, estimated glomerular filtration rate, and CRP. Conversely, the association of TAPSE/PASP ratio with troponin levels may support a predominant role for a direct myocardial injury, reinforced also by the strong association with NT-proBNP.

Although thrombosis and pulmonary embolism have been the subject of interest in explaining, at least in part, the pathophysiology of COVID-19 pulmonary manifestations, we did not find an association between TAPSE/PASP ratio and D-dimer levels, nor with the occurrence of pulmonary embolism. Nonetheless, most patients were receiving anticoagulant therapy.

The average PASP levels in nonsurvivors were only mildly increased (42±12 mm Hg), suggesting that a limited RV adaptability to loading conditions is implicated in the lower TAPSE/PASP ratio, thus indicating that RV dysfunction may occur from the earlier stages of afterload increase.[37] The observed average TAPSE/PASP ratio of 0.48±0.18 mm/mm Hg in nonsurvivors is consistently smaller than the normal reported values of 1.11±0.03 in subjects with a similar mean age,[38] which is relevant because it corroborates the unfavorable

RV-to-Pc coupling in patients with COVID-19 pneumonia, especially in those with worse prognosis. This ratio is markedly reduced similarly to the findings of D'Alto et al in 94 severely ill patients with COVID-19,[6] extending the observations to a wider range of disease severity, because Berlin criteria for ARDS were present in about half of our study population. On the other hand, the identified prognostic cutoff is higher than 0.36, which is highly prognostic in heart failure.[17,39] Overall, these results suggest that in patients with COVID-19, the right heart may fail early and seems oversensitive even to modest increases in the imposed afterload in the context of the COVID-19 pneumonia.

In ROC analysis, the AUC for in-hospital death was 0.75, indicating good accuracy. The best cutoff for predicting in-hospital mortality was a TAPSE/PASP <0.57 mm/mm Hg (75% sensitivity and 70% specificity), similar to the highest combination of sensitivity and specificity found by D'Alto et al in ARDS attributable to COVID-19.[6] Remarkably, in our cohort, patients with TAPSE/PASP<0.57 had a >4-fold increased risk of in-hospital death. At variance with findings of D'Alto et al, we were able to address the TAPSE/PASP ratio in a subset of patients who performed a full echo examination before the COVID-19 infection, based on their planned regular check-up. Interestingly, the differences in TAPSE/PASP ratio provide an argument on the cause–effect relationship between the infection and the observed uncoupling data. In addition, the adverse prognostic effect of RV-to-Pc uncoupling was further explored in the subgroup of patients in whom the quality of echocardiographic images was good enough to obtain 2-dimensional speckle-tracking images, and RV strain parameters were used in place of TAPSE as a surrogate of contractility. We found that both RV GLS/PASP and RV free-wall LS/PASP were strong determinants of in-hospital death, even after multivariable adjustment. The drawback of using strain parameters, potentially highly precise, is that they were feasible in less than half of the study population and required dedicated software and expertise. Despite the challenging setting, TAPSE/PASP ratio was feasible in a slightly higher proportion of patients. Furthermore, this index was easy to calculate at the bedside in unstable, severely ill respiratory patients without the need for sophisticated software. TAPSE/PASP ratio can be implemented as part of the standard bedside echocardiographic examinations in patients hospitalized for severe COVID-19. Further investigations are needed to understand how echocardiographic results could influence patient management improving the outcomes. Although identifying a possible therapeutic target was not the aim of the present study, we may advance some hypotheses on the clinical implications of our results. Once identified by TAPSE/PASP, high-risk subjects may receive more attention and a closer follow-up. Finally, the finding that a negative prognostic effect of COVID19 may be mediated by an uncoupling of RV to Pc is important to understand the mechanism of damage and highlights the need to implement research on this topic.

Limitations

This is a single-center study including a series of patients undergoing a clinically indicated echocardiogram (9% of total patients hospitalized with COVID-19) and a relatively small sample size. These limitations, however, are common to most studies on patients with COVID-19. Some biomarkers like troponin and NT-proBNP were available only in a subgroup of patients. Less than half of the patients had sufficient image quality to perform strain analysis. Despite this proportion being similar to other studies,[5] we decided to move to ancillary analyses, clearly recognizing that we could not formally explore whether the ratio of RV strain to PASP was superior to TAPSE/PASP ratio in predicting death. PASP was measurable by echocardiography only if there was a detectable tricuspid jet. The limited reliability and accuracy of Doppler echocardiography in estimating true pulmonary pressures is well known and shared by all similar studies.[40] The finding that the results were identical using the atrio-ventricular gradient in place of estimated PASP supports the robustness of our results. The echocardiogram was performed earlier in nonsurvivors compared with survivors; therefore, we could not exclude the effect of a temporal bias, because in acute conditions TAPSE/PASP may not be stable. Similarly, it remains undefined if the results would be different if the TAPSE/PASP were measured at a different time point during the evolving disease. In addition, despite several multivariable adjustments, we may not exclude that prior cardiac history might retain a residual influence on the effect of RV-to-Pc coupling on survival.

At the time the study was performed COVID-19 vaccines were not yet available; therefore, we do not know if our results would be similar, but this certainly may represent a step for the near future. Patients with known cardiovascular diseases or risk factors were not excluded, and these conditions may have influenced RV-to-Pc coupling. Nevertheless, these subjects are the most vulnerable to COVID-19 infection, and their exclusion would hamper the generalizability of the results. We acknowledge that our study was limited to a short follow-up analysis, because we only examined in-hospital mortality.

CONCLUSIONS

In patients hospitalized with COVID-19, the noninvasive echocardiographic assessment of RV-to-Pc coupling by the TAPSE/PASP ratio significantly and

independently adds to the prognostic relevance of the PaO_2/FiO_2 ratio, LVEF, age, and CT lung score. These observations prompt for the integration of bedside echocardiography with the right heart-associated parameters including RV size, function, and PASP in assessing the COVID-19 in-hospital clinical course for improving clinical decision making and refining the prediction of adverse events. Present findings point to a direct link between COVID-19 pneumonia, RV-to-Pc uncoupling, and adverse prognosis. Prespecified studies would be of interest for understanding how much these echocardiographic results can impact on patient management and clinical decision making.

ARTICLE INFORMATION

Received July 12, 2021; accepted January 10, 2022.

Affiliations

Division of Cardiology, Department of Health Sciences, University of Milan School of Medicine, San Paolo University Hospital, Azienda Socio Sanitaria Territoriale Santi Paolo e Carlo, Milan, Italy (F.B., G.S., A.M.V., F.T., F.V., D.S., S.C., M.G.); Division of Cardiology, Department of Diagnostics, Clinical and Public Health Medicine, Policlinico University Hospital of Modena, Modena, Italy (A.B.); and Department of Clinical Sciences and Community Health, University of Milano and Fondazione IRCCS Policlinico di Milano, Milan, Italy (F.T., S.C.).

Sources of Funding

None.

Disclosures

None.

Supplemental Material

Tables S1–S2
Figures S1–S3

REFERENCES

1. Gandhi RT, Lynch JB, Del Rio C. Mild or moderate Covid-19. *N Engl J Med*. 2020;383:1757–1766. doi: 10.1056/NEJMcp2009249
2. Akhmerov A, Marban E. COVID-19 and the heart. *Circ Res*. 2020;126:1443–1455. doi: 10.1161/CIRCRESAHA.120.317055
3. Argulian E, Sud K, Vogel B, Bohra C, Garg VP, Talebi S, Lerakis S, Narula J. Right ventricular dilation in hospitalized patients with COVID-19 infection. *JACC Cardiovasc Imaging*. 2020;13:2459–2461. doi: 10.1016/j.jcmg.2020.05.010
4. Kim J, Volodarskiy A, Sultana R, Pollie MP, Yum B, Nambiar L, Tafreshi R, Mitlak HW, RoyChoudhury A, Horn EM, et al. Prognostic utility of right ventricular remodeling over conventional risk stratification in patients with COVID-19. *J Am Coll Cardiol*. 2020;76:1965–1977. doi: 10.1016/j.jacc.2020.08.066
5. Bleakley C, Singh S, Garfield B, Morosin M, Surkova E, Mandalia MS, Dias B, Androulakis E, Price LC, McCabe C, et al. Right ventricular dysfunction in critically ill COVID-19 ARDS. *Int J Cardiol*. 2021;327:251–258. doi: 10.1016/j.ijcard.2020.11.043
6. D'Alto M, Marra AM, Severino S, Salzano A, Romeo E, De Rosa R, Stagnaro FM, Pagnano G, Verde R, Murino P, et al. Right ventricular-arterial uncoupling independently predicts survival in COVID-19 ARDS. *Crit Care*. 2020;24:670. doi: 10.1186/s13054-020-03385-5
7. Bursi F, Santangelo G, Sansalone D, Valli F, Vella AM, Toriello F, Barbieri A, Carugo S. Prognostic utility of quantitative offline 2D-echocardiography in hospitalized patients with COVID-19 disease. *Echocardiography*. 2020;37:2029–2039. doi: 10.1111/echo.14869
8. Li Y, Li HE, Zhu S, Xie Y, Wang B, He L, Zhang D, Zhang Y, Yuan H, Wu C, et al. Prognostic value of right ventricular longitudinal strain in patients with COVID-19. *JACC Cardiovasc Imaging*. 2020;13:2287–2299. doi: 10.1016/j.jcmg.2020.04.014
9. Jones AE, Trzeciak S, Kline JA. The sequential organ failure Assessment score for predicting outcome in patients with severe sepsis and evidence of hypoperfusion at the time of emergency department presentation. *Crit Care Med*. 2009;37:1649–1654. doi: 10.1097/CCM.0b013e31819def97
10. Force ADT, Ranieri VM, Rubenfeld GD, Thompson BT, Ferguson ND, Caldwell E, Fan E, Camporota L, Slutsky AS. Acute respiratory distress syndrome: the berlin definition. *JAMA*. 2012;307:2526–2533. doi: 10.1001/jama.2012.5669
11. Levey AS, Stevens LA, Schmid CH, Zhang Y(, Castro AF, Feldman HI, Kusek JW, Eggers P, Van Lente F, Greene T, et al. A new equation to estimate glomerular filtration rate. *Ann Intern Med*. 2009;150:604–612. doi: 10.7326/0003-4819-150-9-200905050-00006
12. Chung M, Bernheim A, Mei X, Zhang N, Huang M, Zeng X, Cui J, Xu W, Yang Y, Fayad ZA, et al. CT imaging features of 2019 novel coronavirus (2019-nCoV). *Radiology*. 2020;295:202–207. doi: 10.1148/radiol.2020200230
13. Kaminski A, Payne A, Roemer S, Ignatowski D, Khandheria BK. Answering to the call of critically Ill patients: limiting sonographer exposure to COVID-19 with focused protocols. *J Am Soc Echocardiogr*. 2020;33:902–903. doi: 10.1016/j.echo.2020.05.006
14. Kirkpatrick JN, Mitchell C, Taub C, Kort S, Hung J, Swaminathan M. ASE statement on protection of patients and echocardiography service providers during the 2019 novel coronavirus outbreak: endorsed by the American college of cardiology. *J Am Coll Cardiol*. 2020;75:3078–3084. doi: 10.1016/j.jacc.2020.04.002
15. Goldberg AB, Kyung S, Swearingen S, Rao A. Expecting the unexpected: Echo laboratory preparedness in the time of COVID-19. *Echocardiography*. 2020;37:1272–1277. doi: 10.1111/echo.14763
16. Rudski LG, Lai WW, Afilalo J, Hua L, Handschumacher MD, Chandrasekaran K, Solomon SD, Louie EK, Schiller NB. Guidelines for the echocardiographic assessment of the right heart in adults: a report from the American Society of Echocardiography endorsed by the European Association of Echocardiography, a registered branch of the European Society of Cardiology, and the Canadian Society of Echocardiography. *J Am Soc Echocardiogr*. 2010;23(7):685–713;quiz 786–8. doi: 10.1016/j.echo.2010.05.010
17. Guazzi M, Bandera F, Pelissero G, Castelvecchio S, Menicanti L, Ghio S, Temporelli PL, Arena R. Tricuspid annular plane systolic excursion and pulmonary arterial systolic pressure relationship in heart failure: an index of right ventricular contractile function and prognosis. *Am J Physiol Heart Circ Physiol*. 2013;305:H1373–H1381. doi: 10.1152/ajpheart.00157.2013
18. Lang RM, Badano LP, Mor-Avi V, Afilalo J, Armstrong A, Ernande L, Flachskampf FA, Foster E, Goldstein SA, Kuznetsova T, et al. Recommendations for cardiac chamber quantification by echocardiography in adults: an update from the American Society of Echocardiography and the European Association of Cardiovascular Imaging. *J Am Soc Echocardiogr*. 2015;28(1–39):e14. doi: 10.1016/j.echo.2014.10.003
19. Mor-Avi V, Lang RM, Badano LP, Belohlavek M, Cardim NM, Derumeaux G, Galderisi M, Marwick T, Nagueh SF, Sengupta PP, et al. Current and evolving echocardiographic techniques for the quantitative evaluation of cardiac mechanics: ASE/EAE consensus statement on methodology and indications endorsed by the Japanese Society of Echocardiography. *J Am Soc Echocardiogr*. 2011;24:277–313. doi: 10.1016/j.echo.2011.01.015
20. Guazzi M, Naeije R. Right heart phenotype in heart failure with preserved ejection fraction. *Circ Heart Fail*. 2021;14:e007840. doi: 10.1161/CIRCHEARTFAILURE.120.007840
21. Vonk-Noordegraaf A, Haddad F, Chin KM, Forfia PR, Kawut SM, Lumens J, Naeije R, Newman J, Oudiz RJ, Provencher S, et al. Right heart adaptation to pulmonary arterial hypertension: physiology and pathobiology. *J Am Coll Cardiol*. 2013;62:D22–33. doi: 10.1016/j.jacc.2013.10.027
22. Tello K, Wan J, Dalmer A, Vanderpool R, Ghofrani HA, Naeije R, Roller F, Mohajerani E, Seeger W, Herberg U, et al. Validation of the tricuspid annular plane systolic excursion/systolic pulmonary artery pressure ratio for the assessment of right ventricular-arterial coupling in severe pulmonary hypertension. *Circ Cardiovasc Imaging*. 2019;12:e009047. doi: 10.1161/CIRCIMAGING.119.009047

23. Ghio S, Temporelli PL, Klersy C, Simioniuc A, Girardi B, Scelsi L, Rossi A, Cicoira M, Tarro Genta F, Dini FL. Prognostic relevance of a non-invasive evaluation of right ventricular function and pulmonary artery pressure in patients with chronic heart failure. *Eur J Heart Fail*. 2013;15:408–414. doi: 10.1093/eurjhf/hfs208
24. Iacoviello M, Monitillo F, Citarelli G, Leone M, Grande D, Antoncecchi V, Rizzo C, Terlizzese P, Romito R, Caldarola P, et al. Right ventriculo-arterial coupling assessed by two-dimensional strain: a new parameter of right ventricular function independently associated with prognosis in chronic heart failure patients. *Int J Cardiol*. 2017;241:318–321. doi: 10.1016/j.ijcard.2017.04.051
25. Guazzi M, Dixon D, Labate V, Beussink-Nelson L, Bandera F, Cuttica MJ, Shah SJ. RV contractile function and its coupling to pulmonary circulation in heart failure with preserved ejection fraction: stratification of clinical phenotypes and outcomes. *JACC Cardiovasc Imaging*. 2017;10:1211–1221. doi: 10.1016/j.jcmg.2016.12.024
26. Guazzi M. Use of TAPSE/PASP ratio in pulmonary arterial hypertension: an easy shortcut in a congested road. *Int J Cardiol*. 2018;266:242–244. doi: 10.1016/j.ijcard.2018.04.053
27. Lyhne MD, Kabrhel C, Giordano N, Andersen A, Nielsen-Kudsk JE, Zheng H, Dudzinski DM. The echocardiographic ratio tricuspid annular plane systolic excursion/pulmonary arterial systolic pressure predicts short-term adverse outcomes in acute pulmonary embolism. *Eur Heart J Cardiovasc Imaging*. 2021;22:285–294. doi: 10.1093/ehjci/jeaa243
28. Sanz J, Sanchez-Quintana D, Bossone E, Bogaard HJ, Naeije R. Anatomy, function, and dysfunction of the right ventricle: JACC State-of-the-art review. *J Am Coll Cardiol*. 2019;73:1463–1482.
29. Lambermont B, Ghuysen A, Kolh P, Tchana-Sato V, Segers P, Gerard P, Morimont P, Magis D, Dogne JM, Masereel B, et al. Effects of endotoxic shock on right ventricular systolic function and mechanical efficiency. *Cardiovasc Res*. 2003;59:412–418. doi: 10.1016/S0008-6363(03)00368-7
30. Pagnamenta A, Dewachter C, McEntee K, Fesler P, Brimioulle S, Naeije R. Early right ventriculo-arterial uncoupling in borderline pulmonary hypertension on experimental heart failure. *J Appl Physiol*. 1985;2010(109):1080–1085. doi: 10.1152/japplphysiol.00467.2010
31. Park JF, Banerjee S, Umar S. In the eye of the storm: the right ventricle in COVID-19. *Pulm Circ*. 2020;10:2045894020936660.
32. Becker RC. COVID-19 update: Covid-19-associated coagulopathy. *J Thromb Thrombolysis*. 2020;50:54–67. doi: 10.1007/s11239-020-02134-3
33. Klok FA, Kruip M, van der Meer N, Arbous MS, Gommers D, Kant KM, Kaptein F, van Paassen J, Stals M, Huisman MV, et al. Incidence of thrombotic complications in critically ill ICU patients with COVID-19. *Thromb Res*. 2020;191:145–147. doi: 10.1016/j.thromres.2020.04.013
34. Moore JB, June CH. Cytokine release syndrome in severe COVID-19. *Science*. 2020;368:473–474. doi: 10.1126/science.abb8925
35. Chen L, Li X, Chen M, Feng Y, Xiong C. The ACE2 expression in human heart indicates new potential mechanism of heart injury among patients infected with SARS-CoV-2. *Cardiovasc Res*. 2020;116:1097–1100. doi: 10.1093/cvr/cvaa078
36. Hendren NS, Drazner MH, Bozkurt B, Cooper LT Jr. Description and proposed management of the acute COVID-19 cardiovascular syndrome. *Circulation*. 2020;141:1903–1914. doi: 10.1161/CIRCULATIONAHA.120.047349
37. Ling LF, Marwick TH. Echocardiographic assessment of right ventricular function: how to account for tricuspid regurgitation and pulmonary hypertension. *JACC Cardiovasc Imaging*. 2012;5:747–753. doi: 10.1016/j.jcmg.2011.08.026
38. Ferrara F, Rudski LG, Vriz O, Gargani L, Afilalo J, D'Andrea A, D'Alto M, Marra AM, Acri E, Stanziola AA, et al. Physiologic correlates of tricuspid annular plane systolic excursion in 1168 healthy subjects. *Int J Cardiol*. 2016;223:736–743. doi: 10.1016/j.ijcard.2016.08.275
39. Gorter TM, van Veldhuisen DJ, Voors AA, Hummel YM, Lam CSP, Berger RMF, van Melle JP, Hoendermis ES. Right ventricular-vascular coupling in heart failure with preserved ejection fraction and pre- vs. post-capillary pulmonary hypertension. *Eur Heart J Cardiovasc Imaging*. 2018;19:425–432. doi: 10.1093/ehjci/jex133
40. Ciurzyński M, Kurnicka K, Lichodziejewska B, Kozłowska M, Pływaczewska M, Sobieraj P, Dzikowska-Diduch O, Goliszek S, Bienias P, Kostrubiec M, et al. Tricuspid regurgitation peak gradient (TRPG)/Tricuspid Annulus Plane Systolic Excursion (TAPSE) – a novel parameter for stepwise echocardiographic risk stratification in normotensive patients with acute pulmonary embolism. *Circ J*. 2018;82:1179–1185. doi: 10.1253/circj.CJ-17-0940

Supplemental Material

Table S1. Patients' characteristics in the 86 subjects in whom TAPSE/PASP was measurable stratified by TAPSE/PAPS ≥ or <0.57

Variable	TAPSE/PAPS≥0.57 (N=51)	TAPSE/PAPS<0.57 (N=35)	p-value
Age, years	67±13	72±12	0.062
Male sex, n (%)	31(61)	22 (63)	0.846
Weight, Kg	76±15	70±17	0.096
BSA, m^2	1.9±0.2	1.8±0.2	0.174
Caucasian, n (%)	42 (82)	30 (86)	0.678
Risk factors and history			
Smoking, n (%)	10 (22)	14 (41)	0.061
Hypertension, n (%)	25 (49%)	24 (69%)	0.072
Diabetes, n (%)	15 (29%)	6 (17%)	0.193
Previous cardiac disease, n (%)	10 (20%)	25 (71%)	**<0.001**
History of coronary disease, n (%)	6 (12%)	11 (34%)	0.025
History of Heart Failure, n (%)	1 (2)	11 (31)	**<0.001**
Previous valve disease n (%)	1 (2)	10 (29)	**<0.001**
Atrial Fibrillation, n (%)	5 (10)	11 (31%)	**0.011**
ACE or ARB before admission, n (%)	16 (32)	17 (49)	0.123
History of cancer, n (%)	5 (10)	7 (20)	0.180
Chronic obstructive pulmonary disease, n (%)	5 (10)	8 (23)	0.097
Previous stroke, n (%)	2 (4)	3 (9)	0.365
In Hospital therapy			
Corticosteroids, n (%)	33 (66)	22 (65)	0.903
Prophylactic anticoagulants, n (%) Therapeutic anticoagulants, n (%)	28 (55) 21 (41)	11 (31) 21 (60)	0.091
Hydroxychloroquine, n (%)	15 (29)	11 (31)	0.841
Monoclonal antibodies, n (%)	1 (2)	2 (6)	0.754
Antivirals, n (%)	8 (16)	4 (11)	0.576
Immunosuppressants, n (%)	4 (8)	0	0.142
Antibiotics, n (%)	37 (73)	26 (74)	0.858
Presentation			
ARDS by Berlin criteria n (%)	21 (41)	12 (35)	0.586
Type of ventilation None	7 (14%)	5 (14%)	0.688

Nasal cannula Face mask CPAP Bilevel Intubated	6 (12%) 13 (26%) 19 (37%) 1 (2%) 5 (10%)	5 (14%) 12 (34%) 8 (23%) 0 5 (14%)	
CT total severity lung score	8.9±5.6	11±7	0.181
SOFA score	2.4±2.2	2.7±1.9	0.536
HR, bpm	82±14	90±19	0.032
Respiratory rate, breath per minute	21±6	23±8	0.182
Systolic blood pressure, mmHg	127±19	124±26	0.556
Diastolic blood pressure, mmHg	72±12	72±14	0.811
Pulmonary embolism, n (%)	6 (12)	1(3)	0.147
Laboratory data			
Oxygen Saturation, %	97±3	96±4	0.103
PaO_2/FiO_2	246±142	133±23	0.859
PaO_2, mmHg	109±60	106±50	0.766
FiO_2, %	50±23	48±24	0.724
pCO_2, mmHg	38±6	37±8	0.279
pH	7.4±0.05	7.4±0.08	0.407
Creatinine, mg/dl (reference range 0.52-1.04)	0.7 (0.5-0.9)	1.0 (0.8-1.5)	<0.001
eGFR-EPI, mL/m ml/min	95 (83-112)	71 (37-94)	**<0.001**
Troponin I, ng/dl (reference range < 0.034)	0.012 (0.012-0.35)	0.050 (0.016-0.162)	**0.010**
NT-proBNP, pg/ml (reference range 0-296)	828 (361-2550)	9450 (3480-40850)	**<0.001**
Lymphocytes, ($x10^3/\mu L$) (reference range 1-3.4 $x10^3/\mu L$)	1.1 (0.8-1.4)	1.0 (0.6-1.5)	0.566
Lymphocytes, % (reference range 27-37)	14.7 (10.4-24.1)	11 (6.4-17.7)	**0.012**
Neutrophils, $x10^3/\mu L$) (reference range 1.5-7.5)	5.3 (3.6-7.2)	7.4 (4.8-10.4)	**0.008**
Neutrophils, % (reference range 44-74)	71.9 (62.3-83.8)	76.8 (69.1-87.10)	0.069
Ferritin, ng/ml	367 (135-725)	370 (134-769)	0.924
D-dimer, ng/ml (reference range < 270)	619 (320-1845)	787 (499-1913)	0.325
AST, U/L	32 (25-43)	38 (27-57)	0.070

(reference 17-50)			
ALT, U/L (reference < 50)	27 (20-48)	34 (22-83)	0.094
CRP, mg/L (reference range <10)	46 (17-101)	43 (20-729)	0.868
Duration of hospitalization, days	29±17	24±18	0.307
Echocardiographic data			
VTDi, ml/m2	50±18	57±23	0.118
VTSi, ml/m2,	22±11	34±22	0.005
LVEF, %	58±7	44±15	<0.001
WMSI	1.0±0.2	1.5±0.5	<0.001
LV GLS, %	17±3	10±5	<0.001
LAVi, ml/m2	31±11	51±32	0.001
Left Atrial strain, %	22±7	13±7	<0.001
RV diameter, mm	34±5	37±7	0.059
FAC, %	42±5	37±9	0.008
PASP, mmHg	29±8	45±12	<0.001
TAPSE, mm	23±4	17±4	<0.001
TAPSE/PASP, mm/mmHg	0.8±0.3	0.4±0.1	<0.001
RV GLS, %	17±4	13±4	<0.001
RV free-wall LS	20±4	15±4	<0.001

Table S2. Univariate and multivariable cox models for TAPSE/PASP and TAPSE/right atrial-ventricular gradient, mm/mmHg and risk of in-hospital mortality.

	HR for 0.1 mm/mmHg TAPSE/ right atrial-ventricular gradient increase (95%CI)	p-value	HR for 0.1 mm/mmHg TAPSE/PASP increase (95%CI)	p-value
Unadjusted model (n=84)	0.78 (0.66-0.92)	0.003	0.73 (0.59-0.89)	0.003
Model 1 (n=80): adjusted for age and PaO_2/FiO_2	0.72 (0.60-0.87)	0.001	0.66 (0.52-0.84)	0.001
Model 2 (n=80): adjusted for age, PaO_2/FiO_2, and EF	0.76 (0.63-0.93)	0.008	0.71 (0.55-0.93)	0.012
Model 3 (n=69): adjusted for age, PaO_2/FiO_2, and CT lung score	0.77 (0.62-0.94)	0.013	0.72 (0.54-0.94)	0.017

Figure S1. ROC curve for TAPSE/PASP.

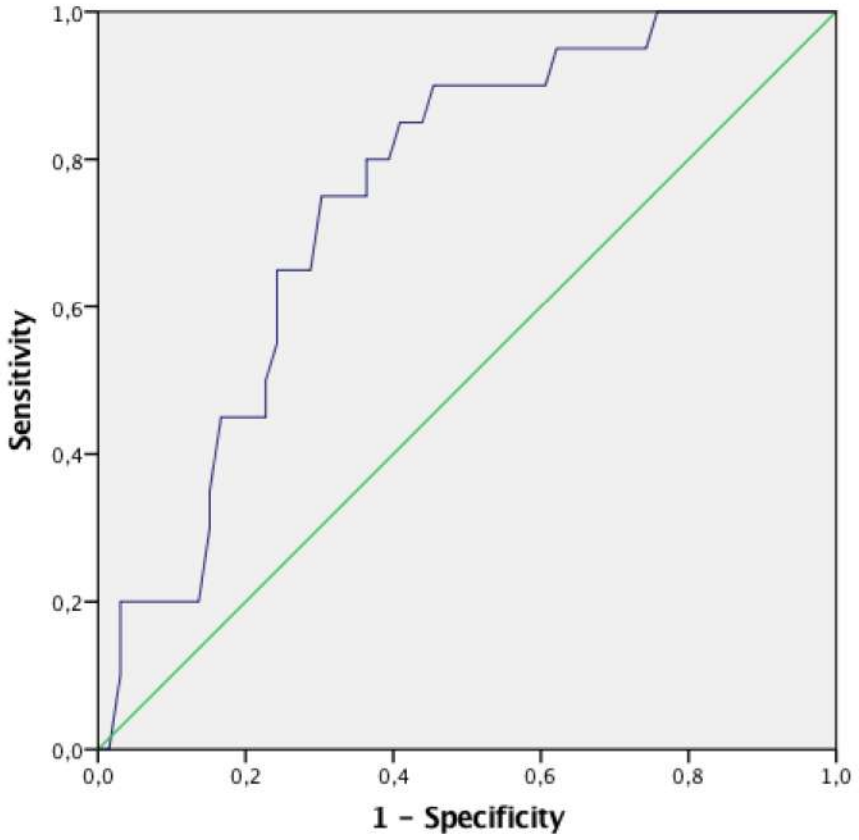

Cut point of ROC	corresponding specificity	corresponding sensitivity
<0.571 mm/mmHg	70%	75%
<0.595 mm/mmHg	80%	64%
<0.656 mm/mmHg	90%	54%

Figure S2. ROC curve for RV free-wall LS/PASP.

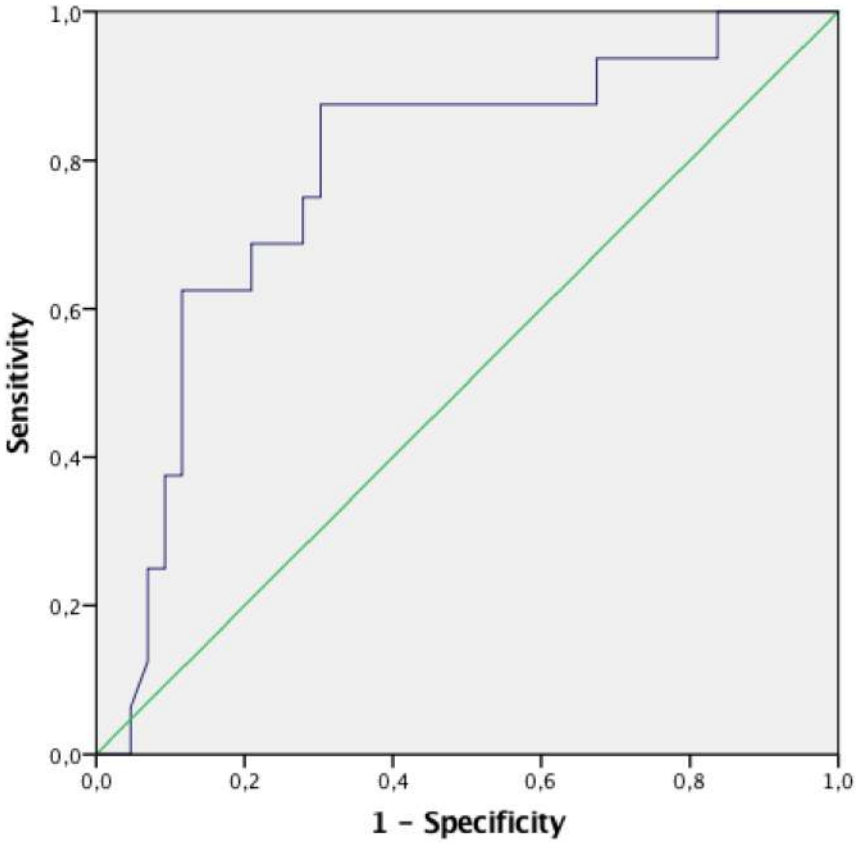

Figure S3. ROC curve for RV GLS/PASP.